The Cryosphere Discuss., 6, 1531–1562, 2012
www.the-cryosphere-discuss.net/6/1531/2012/
doi:10.5194/tcd-6-1531-2012


The Cryosphere Discussions



# Sensitivity of Greenland Ice Sheet surface mass balance to surface albedo parameterization: a study with a regional climate model

**J. H. van Angelen[1], J. T. M. Lenaerts[1], S. Lhermitte[2], X. Fettweis[3], P. Kuipers Munneke[1], M. R. van den Broeke[1], and E. van Meijgaard[2]**

[1]Institute for Marine and Atmospheric Research Utrecht, Utrecht University, The Netherlands
[2]Royal Netherlands Meteorological Institute, De Bilt, The Netherlands
[3]Department of Geography, University of Liège, Belgium

Received: 5 April 2012 – Accepted: 12 April 2012 – Published: 24 April 2012

Correspondence to: J. H. van Angelen (j.h.vanangelen@uu.nl)

Published by Copernicus Publications on behalf of the European Geosciences Union.

## Abstract

We present a sensitivity study of the surface mass balance (SMB) of the Greenland Ice Sheet, as modeled using a regional atmospheric climate model, to various parameter settings in the albedo parameterization. The snow albedo parameterization uses grain size as a prognostic variable and further depends on cloud cover, solar zenith angle and black carbon concentration. For the control experiment the overestimation of absorbed shortwave radiation (+6 %) at the K-transect (West Greenland) for the period 2004–2009 is considerably reduced compared to the previous density-dependent albedo parameterization (+22 %). To simulate realistic snow albedo values, a small concentration of black carbon is needed. A background ice albedo field derived from MODIS imagery improves the agreement between the modeled and observed SMB gradient along the K-transect. The effect of enhanced retention and refreezing is a decrease of the albedo due to an increase in snow grain size. As a secondary effect of refreezing the snowpack is heated, enhancing melt and further lowering the albedo. Especially in a warmer climate this process is important, since it reduces the refreezing potential of the firn layer covering the Greenland Ice Sheet.

## 1 Introduction

Mass loss from the Greenland Ice Sheet (GrIS) is expected to become a major contributor to sea level rise this century (IPCC-AR4). After a 30 yr period (1960–1990) during which the GrIS was in approximate mass balance (i.e., the mass gain by precipitation was approximately equal to the mass loss by surface runoff and ice discharge), the mass balance has turned negative in the last 20 yr, with a larger melt extent (Fettweis et al., 2011), increasing surface runoff (Ettema et al., 2009; Hanna et al., 2008) and increased glacier discharge (Nick et al., 2009; Rignot et al., 2011). In the last decade, the contributions made to the total mass loss of ~ 2400 Gt, were for ~ 60 % accounted for by enhanced runoff and for ~ 40 % by enhanced discharge (Van den Broeke et al., 2009; Rignot et al., 2008). With outlet glaciers retreating and near surface air temperature increasing further, mass loss in the near future will likely remain dominated by surface runoff.

The most important energy source for surface runoff is the absorption of solar radiation (Van den Broeke et al., 2008a), which is mainly determined by cloud cover and surface albedo. Modeled surface mass balance (SMB) of the GrIS is highly sensitive to surface albedo (Bougamont and Bamber, 2005; Fitzgerald et al., 2012; Tedesco et al., 2011), owing to the positive melt-albedo feedback, which results in lower albedos in high-melt years (Stroeve, 2007). Following recent warming, a persistent drop in albedo has been observed in satellite data and climate models (Box et al., 2012).

Any physically-based approach to project future GrIS mass blance requires a high resolution climate model that represents surface albedo adequately, including all processes that influence its evolution (Bougamont et al., 2007). For a proper interpretation of SMB projections it is essential to understand the physical processes in the snowpack, their influence on albedo and ultimately on the surface mass balance.

In this paper we address the sensitivity of the SMB of the GrIS to changes in the different parameter settings of a particular albedo parameterization scheme. For this we use the high resolution climate model RACMO2 (Van Meijgaard et al., 2008; Ettema et al., 2010a), recently extended with a new albedo parameterization scheme (Kuipers Munneke et al., 2011). The next section will briefly describe in situ albedo observations, RACMO2 and the albedo parameterization and lists the sensitivity tests performed in this study. Results are discussed in Sect. 3 and conclusions and a future outlook is given in Sect. 4.

## 2 Data and methods

### 2.1 AWS observations

Since 1990, the Institute for Marine and Atmospheric research Utrecht (IMAU) has performed mass balance and meteorological measurements along a transect (Kangerlussuaq transect or K-transect), located on the western margin of the GrIS at 67° N (Van de Wal et al., 2005). The ablation area here is up to 150 km wide with gentle slopes, representing the largest ablation region of the GrIS. In August 2003, three automatic weather stations were installed along the transect (Van den Broeke et al., 2008a), indicated by the three black dots in the inset of Fig. 1. The measurements of incoming and outgoing shortwave radiation are used for evaluation of RACMO2. The lowest station (S5) is located ∼ 5 km from the ice sheet margin at an altitude of 420 m. This site experiences an average mass loss of ∼ 3.5 m of water equivalent (m w.e.) per year. Station S6 is located ∼ 40 km from the margin, at an altitude of approximately 1000 m, in rough terrain with melt water channels in summer (Fig. 2a) and an average mass loss of ∼ 2 m w.e. $\mathrm{yr}^{-1}$. Station S9 (Fig. 2b) is situated ∼ 80 km from the margin, at an altitude of around 1500 m. At the onset of the stake measurements, S9 was close to the equilibrium line, but in the most recent 5 yr an average mass loss of 0.5 m w.e. $\mathrm{yr}^{-1}$ has been observed here. In this study only data from stations S6 and S9 are used, because S5 is located on the outlet of Russell Glacier, which is not resolved in RACMO2.

### 2.2 Melt days

As a second evaluation method, we use the amount of melting days in the summer of 2007 based on satellite retrievals. Daily values of brightness temperature from the Special Sensor Microwave/Imager (SSM/I) F-13 (1995–2009) are regridded on a 25 × 25 km EASE-grid, as distributed by the National Snow and Ice Data Center (Armstrong and Brodzik, 1995). The brightness temperatures are derived as in Abdalati and Steffen





TCD
6, 1531–1562, 2012

(1997, 2001). As a threshold to determine whether melt is present a brightness temperature of 227.5 K is used, see Fettweis et al. (2011).

### 2.3 Regional atmospheric climate model

We use the Regional Atmospheric Climate Model (RACMO2) (Van Meijgaard et al., 2008), developed by the Royal Netherlands Meteorological Institute (KNMI). Over the last decade, RACMO2 has been adapted to realistically simulate ice sheet SMB by the implementation of a multilayer snow model (Ettema et al., 2010a) and a drifting snow scheme (Lenaerts et al., 2010). In this study RACMO2 is applied with a horizontal grid spacing of approximately 11 km and 40 sigma levels in the vertical. The domain covers Greenland and its surrounding seas, including the Canadian Arctic Archipelago, Iceland and Svalbard (Fig. 1). At the lateral boundaries RACMO2 is forced every 6 h by ERA-Interim reanalysis data (Simmons et al., 2007). At the surface boundary sea surface temperature and sea ice extent are prescribed. Ettema et al. (2010a,b) evaluated RACMO2 for the period 1958–2008 over Greenland. Recently, output of RACMO2 has been successfully used to solve for the total mass budget of the GrIS (Van den Broeke et al., 2009), to describe the momentum budget of the katabatic boundary layer (Van Angelen et al., 2011a) and to explain the wind-driven sea-ice export through Fram Strait (Van Angelen et al., 2011b).

### 2.4 Albedo parameterization

The most important physical property influencing snow albedo is snow grain size (Wiscombe and Warren, 1980): larger grains are both more absorptive and scatter solar radiation preferentially in the forward direction, into the snowpack, enhancing the chances that photons are absorbed. Clouds, solar zenith angle and impurities due to soot and dust also have an impact on the albedo. In previous model versions of RACMO2, broadband albedo was snow density-dependent (Greuell and Konzelmann, 1994). Although the density of snow is a measure for snow metamorphism, as it increases with increasing grain size, a density dependent albedo scheme is unphysical (Wiscombe and Warren, 1980). Especially for wet snow conditions, a density dependent albedo parameterization tends to underestimate albedo, resulting in an overestimation of absorbed solar radiation, and consequently a too early and too long exposure of bare ice at the surface (Ettema et al., 2010a). Figure 3 compares measured and modeled albedo at S9, using the previous, density dependent albedo scheme. In reality, only for a short period in August bare ice was present at the surface, whereas the modeled albedo predicts ice at the surface from mid July until the end of September. Too low albedos in June resulted in a rapid melt of the snowcover.

The new albedo parameterization as implemented in RACMO2 is discussed in Kuipers Munneke et al. (2011), who discusses its successful implementation in RACMO2 for the Antarctic ice sheet. The new albedo scheme is based on the parameterization developed by Gardner and Sharp (2010), in which a broadband albedo is calculated depending on snow grain size, solar zenith angle, cloud cover and contamination of the snowpack by black carbon:

$$\alpha = \alpha_S + d\alpha_u + d\alpha_c + d\alpha_\tau. \tag{1}$$

The final broadband albedo ($\alpha$) is the sum of a base albedo ($\alpha_S$) that depends on snow grain size, corrected for solar zenith angle ($d\alpha_u$), contamination ($d\alpha_c$) and clouds ($d\alpha_\tau$). Solar zenith angle and cloud cover are readily available from RACMO2. Kuipers Munneke et al. (2011) introduced a new prognostic variable in RACMO2, the effective snow grain size ($r_e$). The effective snow grain size itself is a mass weighted average of the snow grain size of fresh snow ($f_n$), old snow ($f_o$) and refrozen liquid water ($f_r$) in a snow layer:

$$r_e(t) = [r_e(t-1) + dr_{e,dry} + dr_{e,wet}]f_o + r_{e,0}f_n + r_{e,r}f_r\,. \tag{2}$$

The snow grain size of fresh snow ($r_{e,0}$) and refrozen snow ($r_{e,r}$) is chosen constant in time and space. The grain size of old snow is based on the snow grain size in the previous time step ($r_e(t-1)$) corrected for dry and/or wet snow metamorphism. The ageing of dry snow ($dr_{e,dry}$) is parameterized from the microphysical snow grain growth Snow, Ice, and Aerosol Radiative model (SNICAR) (Flanner and Zender, 2006). Since the complete SNICAR model is computationally too expensive, a parameterization is used that has temperature, temperature gradient and density of the specific snow layer as input. Wet snow metamorphism ($dr_{e,wet}$) is based on Brun et al. (1989), in which the growth of the snow grains is dependent on the amount of liquid water present in the snowpack.

Black carbon concentrations in Antarctic snow are very low (Warren and Clarke, 1990; Grenfell et al., 1994), so a correction for black carbon was not applied by Kuipers Munneke et al. (2011). In contrast, black carbon concentrations of 0.05 ppmv have been measured at Summit (Flanner et al., 2007), Greenland, and probably even higher concentrations are present in the lower regions. This will have a significant impact on snow albedo (Hansen and Nazarenko, 2004; Flanner et al., 2007). The effect of black carbon on broadband snow albedo in RACMO2 follows Eq. (8) in Gardner and Sharp (2010):

$$d\alpha_c = \max\left(0.04 - \alpha_S, \frac{-c^{0.55}}{0.16 + 0.6S^{0.5} + 1.8c^{0.6}S^{-0.25}}\right), \tag{3}$$

in which $S$ is the specific surface area of the snow grains ($m^2\,kg^{-1}$) and $c$ the carbon loading (ppmv). The black line in Fig. 4 shows broadband albedo for a range of snow grains between 20 and 1000 µm, without correcting for black carbon, cloud cover or solar zenith angle. Fresh snow albedo is as high as 0.85, but drops rapidly with increasing snow grain size to a value of 0.7 for 1 mm grains (typical for wet snow). The colored lines show $d\alpha_c$ for three different values of carbon loading: 0.05 ppmv (blue), 0.1 ppmv (green) and 0.2 ppmv (red). The effect of black carbon on albedo increases with increasing grain size. The reason is that photons are preferentially scattered forward by larger grains and thus have a longer pathway in snow with larger grain sizes, increasing the chances to meet a black carbon particle and being absorbed by it. For a snowpack consisting of grains with an average grain size of 1 mm, a carbon loading of 0.1 ppmv will decrease the albedo from 0.7 to 0.63, equivalent to an increase in the absorption of shortwave radiation of 20 %.

### 2.5 MODIS background ice albedo

The albedo of bare ice in the ablation area of the GrIS is not constant in space and time (Box et al., 2012). In the southwestern region of the ice sheet, the so called dark band (Wientjes et al., 2011) shows albedo values < 0.4, while similarly strong spatial albedo variability is found in other parts of the GrIS (Boggild et al., 2010). This motivated us to compile an ice albedo field that can serve as background ice albedo in RAMCO2.

Figure 1 shows the background ice albedo (BIA) field used in the CONTROL simulation. The BIA is used if the density of the top two layers of the snow model is equal to the density of ice (910 $\mathrm{kg\,m^{-3}}$). The BIA is based on the moderate-resolution imaging spectroradiometer (MODIS) white sky albedo product (NASA Land Processes Distributed Active Archive Center (LP DAAC). Albedo 16-day L3 Global 0.05° CMG. USGS/Earth Resources Observation and Science (EROS) Center, Sioux Falls, South Dakota. 2012.). The satellite data are based on a 16 day integration period, with a time resolution of 8 days at a horizontal resolution of 0.05° ($\sim$ 5 km). The MODIS albedo product has been evaluated by Stroeve et al. (2005); MODIS derived albedos are accurate for albedo values < 0.7 over Greenland and as such they are suitable for determining a background ice albedo field.

The BIA field is calculated using 10 yr of MODIS data (2001–2010), taking the average of the lowest 5 % of data at every grid point. A minimum value is set to 0.3, and a maximum to 0.55. The latter value is also used for locations which are snow covered throughout the year, but are expected to become snow free in the coming years. For grid points with missing MODIS data, a problem occurring only at high latitudes (> 80° N), the BIA is set to 0.47, being the average albedo of all the ice points. Note that this value is significantly lower than the ice albedo value of 0.52 used in the previous version of RACMO2 (0.52, Ettema et al., 2010a).





TCD
6, 1531–1562, 2012
Albedo and SMB of Greenland
J. H. van Angelen et al.

Although ice albedos as observed by MODIS are reasonably stable from year to year, some inter-annual variability remains. For example, at the location of S6, the lowest MODIS-derived ice albedo values range between 0.34 and 0.44 in the period 2004–2010. This variability is partly due to measuring uncertainties (mainly due to cloud cover), and partly a real phenomenon, possibly associated with delayed supraglacial runoff of meltwater (Van den Broeke et al., 2008b).

### 2.6 Model experiments

To tune and evaluate the new albedo parameterization, we have performed seven RACMO2 simulations for the year 2007. Performing these experiments is computationally expensive and time consuming, therefore a single year is chosen. The year 2007 is the record melt year in the last decade and thus the best resemblance for future warmer years with an increasing ablation area; important to simulate correctly. Evaluation is done with the emphasis on melt extent and station S9, located close to the equilibrium line where the local SMB is very sensitive to small changes in the albedo scheme. Radiation measurements have been performed at several other locations on the GrIS (Steffen and Box, 2001), but most of them are located in the accumulation area at ~ 2000 m where albedo variations are small.

Table 1 summarizes the different albedo experiments with RACMO2. The ANT settings are the settings used for the Antarctica integration (Kuipers Munneke et al., 2011). With every new experiment one parameter is changed. In FSGRAIN the specific surface area of fresh snow is decreased from 80 to 60 $m^2 kg^{-1}$, equivalent to an increase in effective radius of the grain size ($r_{e,0}$) from 41 to 55 µm. In the previous RACMO2 snow albedo scheme, the maximum amount of liquid water in the snowpack was limited to 2 %. In the new snow albedo scheme, this artificial limit is no longer needed, and the amount of liquid water in the snowpack is calculated following Coléou and Lesaffre (1998). In their expression, the maximum amount of liquid water is related to the available pore space in the snowpack and can reach values of up to 13 % of the weight of the snowpack (experiment LWMAX). Next, in RFGRAIN, the grain size of refrozen





TCD
6, 1531–1562, 2012

snow is increased from 1 to 2 mm, followed in ICEALB by a decrease of the ice albedo from 0.5 to 0.45. In RSOOT black carbon is added to the snowpack (0.1 ppmv), and in the final simulation (CONTROL) MODIS background ice albedos are used instead of a spatially constant value.

## 3 Results

### 3.1 Albedo time series

Figure 5 displays time series of modeled and measured albedo at locations S6 (Fig. 5a) and S9 (Fig. 5b) for the year 2007. In winter the rough ice surface at S6 is snow covered, resulting in albedo values of 0.8–0.9 until the end of May. The thin (∼ 40 cm) snowcover at S6 disappears rapidly and at the beginning of June ice appears at the surface, the timing of this is well simulated in CONTROL. In ANT, melting the snowpack takes two weeks longer, due to a higher snow albedo in spring. In both ANT and CONTROL, the end of the melt season at the end of August is well timed. The background ice albedo in CONTROL is slightly too low compared to the observations (AWS and MODIS) for this specific year.

Results for S9 are displayed in Fig. 5b. In this specific year, bare ice is exposed at the end of June, about two weeks later than at S6. In experiment CONTROL the onset of the melt season is again well timed. In ANT, the snow layer does not fully melt, which emphasizes the fact that close to the equilibrium line, small changes in the albedo can have a strong impact on the surface mass balance. At S9 the background albedo is 0.55, in good agreement with the weather station and the MODIS observations. Note that the snowfall events at the end of June and August are well represented in RACMO2.

Figure 6a compares albedo time series at S9 with MODIS and CONTROL for the period 2004–2009. Overall, RACMO2, the in situ measurements and MODIS observations are in good agreement. Averaged albedo over the months March to September is





TCD
6, 1531–1562, 2012

0.774 (modeled) compared to 0.794 (measured at the AWS). This represents a large improvement compared to the simulation with the density dependent albedo scheme (0.721). In that scheme an artificial minimum snow albedo of 0.7 was imposed to prevent an unrealistic decrease in snow albedo during periods of strong snowmelt. This limit is no longer needed in the new parameterization.

In most years, the MODIS inferred albedo shows a higher minimum albedo compared to both the AWS measurements and the RACMO2 results. MODIS uses a 16 day time span to calculate a single albedo value; the exposure of bare ice at S9 in a regular melt season is seldom continuous for a 16 day period, but interrupted by snowfall events. An exception is the year 2007, where MODIS albedo decreases to values close to 0.55.

Figure 6b depicts measured (red) and modeled (black) net shortwave radiation, Fig. 6c shows the differences. The numbers in Fig. 6c denote the mean bias and root-mean-square error (RMSE) for the individual years. Averaged over the 6 yr period, modeled net shortwave radiation is 3.0 $\mathrm{W\,m^{-2}}$ or 6 % larger than the measured values. This discrepancy can be ascribed mainly to the two years 2004 and 2005 where the albedos in spring (May) are underestimated. This result compares favorably to the offset in the simulation with the previous, density-dependent albedo scheme (11.4 $\mathrm{W\,m^{-2}}$).

The RMSEs are on average 24.0 $\mathrm{W\,m^{-2}}$, which, compared to the average mean bias, is still significant. This remains a consequence of carrying out climate simulations, because the exact timing of snowfall events remains difficult. However, it is important to simulate the average net radiation correctly, such that the right amount of energy is available for melting and a correct estimate of snow melt is obtained.

### 3.2 SMB components

To assess the effect of the individual experiments on snow melt, the total number of melt days for the period according to SSMI brightness temperatures is displayed in Fig. 7a, and for the RACMO2 simulations in Fig. 7b–h. Figure 8 shows the percentage increase of melt in a new simulation compared to the preceding simulation in Table 1.





TCD
6, 1531–1562, 2012

Table 2 lists SMB and its components for the seven simulations for calendar year 2007, integrated over the entire GrIS.

In all simulations, total precipitation is around 715 Gt of which 50 ± 3 Gt (7 %) falls as rain. The ANT run shows a total sublimation of 27 Gt and 340 Gt melt. 156 Gt (40 %) of the available liquid water refreezes in the snowpack, and 242 Gt runs off as meltwater, resulting in a positive surface mass balance of 444 Gt, two-third of the total mass gained by precipitation. For the year 2007, this value for total SMB is too high (Van den Broeke et al., 2009). The lack of melt is reflected in the number of melt days for the period March to April 2007 compared to SSMI (Fig. 7).

Increasing the snow grain size of fresh snow from 41 to 55 µm ("FSGRAIN" simulation), results in an increase in melt to 374 Gt (+10 %). The additional liquid water flux is equally divided between refreezing and runoff, resulting in a SMB decrease of 29 Gt (−7 %). Figure 8a shows that a larger grain size for fresh snow results in ~ 30 % more melt in the accumulation area in south Greenland. An increase in grain size also results in an earlier start of the melt season and hence the earlier appearance of bare ice in the ablation region, leading to a ~ 10 % increase in melt in ablation areas.

Changing the maximum liquid water content in the snowpack, from 2 % to a value determined by the scheme of Coléou and Lesaffre (1998) ("LWMAX" simulation in Table 2), hardly affects the total SMB, although individual SMB components show significant variations. The larger amount of liquid water allowed to be retained in the snowpack facilitates refreezing; this increases snow grain size, accompanied by a decrease in the albedo and resulting in ~ 9 % more snow melt, with locally an increase of up to 50 % in the south (Fig. 8b). Due to the larger retention capacity, a significant amount of liquid water is still present in the snowpack at the end of September (~ 20 Gt). So although the change in the snowpack physics does not alter the SMB directly, the extra snow melt and refreezing will cause the snowpack to warm and probably results in extra melt in the following year. The number of melt days also increases (Fig. 7d), but is still too small compared to the satellite data (Fig. 7a).

Increasing the grain size of refrozen snow from 1 to 2 mm (RFGRAIN) has a strong impact on the SMB (−48 Gt or −12 %). Snowmelt increases by almost 20 %, most of which runs off the ice sheet. In some areas the amount of snow melt more than doubles (Fig. 8c). It is interesting to note that changes in the refreezing parameters (LWMAX and RFGRAIN) have most impact on melt in regions higher up the ice sheet and along the southeast coast, where precipitation rates are high, because in those regions the full refreezing capacity of the snowpack is not reached.

A decrease of the ice albedo from 0.5 to 0.45 ("ICEALB" simulation) is equivalent to an extra uptake of shortwave radiation by 10 % if bare ice is present at the surface. This increases total melt by another 23 Gt or 5 %. Since only areas are affected where bare ice is at the surface, runoff increases by the same amount. The 10 % increase in melt (Fig. 8d) in regions with bare ice at the surface, equals the increase in net shortwave radiation, which is in agreement with Van den Broeke et al. (2008a), who showed that temporal variability in melt in the western ablation region of the GrIS is mainly driven by variability in shortwave radiation. In the future it is expected that SMB sensitivity to the background ice albedo will increase, since on average a larger area of bare ice will be present at the surface for a longer period each year (Fettweis et al., 2011). The relatively small differences in the accumulation zone in Fig. 8d cancel out in the mean and are due to small changes in the snowfall pattern in the different simulations.

In RSOOT we added 0.1 ppmv of black carbon to the snowpack. The direct effect on albedo, as discussed in Sect. 2.4, is displayed in Fig. 4: the albedo of fresh snow is reduced by 0.02 and that of older snow by up to 0.07, equivalent to an extra uptake of shortwave radiation of 10 % and 20 %, respectively. However, the increase in snowmelt is 48 % (+239 Gt), indicating the importance of positive feedbacks. The increase in absorbed shortwave radiation heats the snowpack, resulting in larger snow grains, which in turn lowers the albedo and further enhances the absorption of shortwave radiation. The increase in runoff is larger than the increase in refrozen meltwater, owing to an earlier onset of melting as a result of which bare ice is exposed earlier in the season. The relative effect of black carbon on melt increases gradually with height (Fig. 8e),





TCD
6, 1531–1562, 2012

from ∼ 10 % in the ablation region to over 200 % in the higher accumulation regions. The number of melt days (Fig. 7e) is now on average in good agreement with the satellite measurements (Table 2), although regional differences remain. This demonstrates that a low soot concentration is required to obtain realistic snow albedos.

In the final simulation (CONTROL) the background ice albedo field is applied (see Sect. 2.5). The total amount of melt is slightly reduced, because on average the BIA is 0.47, slightly higher than the value in the preceding simulation (0.45). However, since BIA varies between 0.3 and 0.55, regional changes are significant, e.g. a ∼ 15 % increase in melt in the dark band in the western ablation area (Fig. 8f).

The experiments show that when varied within realistic parameter spaces, the albedo scheme introduces variations in total surface mass balance averaged over the GrIS between +177 and +444 Gt for the year 2007, equivalent to 25 % and 62 % of the total precipitation, respectively. This underlines the strong sensitivity of Greenland SMB to surface albedo. It should be noted that the uncertainty in modeled Greenland SMB is not equally large, because results of the CONTROL experiment are in much better agreement with in situ measurements and satellite observations compared to the other experiments. Furthermore it is difficult to assess the absolute value of SMB, because no direct measurements of meltwater runoff are available. Especially for future projections the changes in SMB components with respect to present day conditions will determine increase in sea level rise, therefore it is more important to simulate the inter-annual variability in SMB correctly than the absolute values (Van den Broeke et al., 2009). Furthermore the inter-annual variability in SMB is more dependent on total accumulation and summer temperatures than on albedo (Ettema et al., 2009).

### 3.3 SMB along the K-transect

Figure 9 compares the averaged observed surface mass balance along the K-transect for the period 1991 to 2010 with results of RACMO2 using the CONTROL settings. The observed SMB ranges from −4 m w.e. at an altitude of 500 m to +0.5 m w.e. at 2000 m. This gradient is well captured by RACMO2. Between 1000 and 1700 m elevation, the total SMB is still somewhat underestimated. This is probably not related to albedo, since the modeled albedo at station S9 (1500 m) is in good agreement to the observed albedo. Ettema et al. (2010a) demonstrated that the sensible heat flux is overestimated at S6 and S9. This problem is still present in the new RACMO2 simulation and presents a plausible explanation for the offset in SMB. As a result, the equilibrium line altitude in RACMO2 (around 1800 m in Fig. 9) is simulated about 200 m too high.

Figure 10 shows strong spatial variability in SMB at a constant altitude. This is directly related to the background albedo field; the blue and green dots in Fig. 10 can be easily linked to each other for the lower ablation region (< 1200 m). As a first approximation, a decrease in background albedo of 0.07 is equivalent to a 0.5 m w.e. lower SMB. The use of a background ice albedo field thus improves the results in the lower ablation region.

## 4 Summary and conclusions

We have used the regional atmospheric climate model RACMO2 to assess the sensitivity of the surface mass balance (SMB) of the GrIS to a new snow albedo parameterization. The snow albedo parameterization uses a prognostic snow grain size and introduces corrections for cloud cover, solar zenith angle and black carbon loading. We also applied a spatially variable background ice albedo field, based on 2000–2010 MODIS satellite retrievals. This affects especially regions with strong ice albedo variability, such as the dark band in the western ablation zone. In situ SMB observations and satellite derived melt duration have been used to evaluate RACMO2 including the new albedo scheme. With the new albedo parameterization, RACMO2 agrees better with albedo measurements at the K-transect in West Greenland. The steep SMB gradient in this region is now well represented compared to the previous, density-dependent albedo scheme.

A complicated and poorly understood process is the interaction between albedo and the refreezing and retention of melt water. Although the direct effect of an increase in the maximum retention capacity of the snowpack on the SMB is small, the indirect effect could be significant, e.g., by warming the snowpack and further enhancement of melting. This process is particularly important in a non-steady warming climate, since it determines the capacity for refreezing of infiltrated meltwater within the firn column. To study this, a high-resolution climate scenario run will be carried out with RACMO2 for the GrIS. Using results from the present study, we expect to be able to provide a more detailed projection of Greenland mass loss and associated sea level rise with a better constrained uncertainty.

*Acknowledgements.* This work was supported by funding from the ice2sea programme from the European Union 7th Framework Programme, grant number 226375. Ice2sea contribution number 084. We would like to thank Paul Smeets and Roderik van de Wal for providing SMB data from the K-transect.

## References

Abdalati, W. and Steffen, K.: Snowmelt on the Greenland ice sheet as derived from passive microwave satellite data, J. Climate, 10, 165–175, doi:10.1175/1520-0442(1997)010<0165:SOTGIS>2.0.CO;2, 1997. 1534

Abdalati, W. and Steffen, K.: Greenland ice sheet melt extent: 1979–1999, J. Geophys. Res., 106, 33983–33988, doi:10.1029/2001JD900181, 2001. 1535

Armstrong, R. and Brodzik, M.: An earth-gridded SSM/I data set for cryospheric studies and global change monitoring, Adv. Space Res., 16, 155–163, doi:10.1016/0273-1177(95)00397-W, 1995. 1534

Boggild, C., Brandt, R., Brown, K., and Warren, S.: The ablation zone in northeast Greenland: ice types, albedos and impurities, J. Glaciol., 56, 101–113, doi:10.3189/002214310791190776, 2010. 1538

Bougamont, M. and Bamber, J. L.: A surface mass balance model for the Greenland Ice Sheet, J. Geophys. Res., 110, F04018, doi:10.1029/2005JF000348, 2005. 1533

Bougamont, M., Bamber, J. L., Ridley, J. K., Gladston, R. M., Greuell, W., Hanna, E., Payne, A. J., and Rutt, I.: Impact of model physics on estimating the surface mass balance of the





Title Page
Abstract Introduction
Conclusions References
Tables Figures
Back Close
Full Screen / Esc
Printer-friendly Version
Interactive Discussion

Greenland ice sheet, Geophys. Res. Lett., 34, L17501, doi:10.1029/2007GL030700, 2007. 1533
Box, J. E., Fettweis, X., Stroeve, J. C., Tedesco, M., Hall, D. K., and Steffen, K.: Greenland ice sheet albedo feedback: thermodynamics and atmospheric drivers, The Cryosphere Discuss., 6, 593–634, doi:10.5194/tcd-6-593-2012, 2012. 1533, 1538
Brun, E., Martin, E., Simon, V., and Gendre, C.: An energy and mass model of snow cover suitable for operational avalanche forecasting, J. Glaciol., 35, 333–342, 1989. 1537
Coléou, C. and Lesaffre, B.: Irreducible water saturation in snow: experimental results in a cold laboratory, Ann. Glaciol., 26, 64–68, 1998. 1539, 1542, 1551
Ettema, J., Van den Broeke, M. R., Van Meijgaard, E., Van de Berg, W. J., Bamber, J. L., Box, J. E., and Bales, R. C.: Higher surface mass balance of the Greenland ice sheet revealed by high-resolution climate modeling, Geophys. Res. Lett., 36, L12501, doi:10.1029/2009GL038110, 2009. 1532, 1544, 1562
Ettema, J., van den Broeke, M. R., van Meijgaard, E., van de Berg, W. J., Box, J. E., and Steffen, K.: Climate of the Greenland ice sheet using a high-resolution climate model – Part 1: Evaluation, The Cryosphere, 4, 511–527, doi:10.5194/tc-4-511-2010, 2010a. 1533, 1535, 1536, 1538, 1545
Ettema, J., van den Broeke, M. R., van Meijgaard, E., and van de Berg, W. J.: Climate of the Greenland ice sheet using a high-resolution climate model – Part 2: Near-surface climate and energy balance, The Cryosphere, 4, 529–544, doi:10.5194/tc-4-529-2010, 2010b. 1535
Fettweis, X., Tedesco, M., van den Broeke, M., and Ettema, J.: Melting trends over the Greenland ice sheet (1958–2009) from spaceborne microwave data and regional climate models, The Cryosphere, 5, 359–375, doi:10.5194/tc-5-359-2011, 2011. 1532, 1535, 1543
Fitzgerald, P. W., Bamber, J. L., Ridley, J. K., and Rougier, J. C.: Exploration of parametric uncertainty in a surface mass balance model applied to the Greenland ice sheet, J. Geophys. Res., 117, F01021, doi:10.1029/2011JF002067, 2012. 1533
Flanner, M. G. and Zender, C. S.: Linking snowpack microphysics and albedo evolution, J. Geophys. Res., 111, D12208, doi:10.1029/2005JD006834, 2006. 1537
Flanner, M. G., Zender, C. S., Randerson, J. T., and Rasch, P. J.: Present-day climate forcing and response from black carbon in snow, J. Geophys. Res., 112, D11202, doi:10.1029/2006JD008003, 2007. 1537

Gardner, A. S. and Sharp, M. J.: A review of snow and ice albedo and the development of a new physically based broadband albedo parameterization, J. Geophys. Res., 115, F01009, doi:10.1029/2009JF001444, 2010. 1536, 1537

Grenfell, T. C., Warren, S. G., and Mullen, P. C.: Reflection of solar radiation by the Antarctic snow surface at ultraviolet, visible and near-infrared wavelengths, J. Geophys. Res., 99, 18669–18684, doi:10.1029/94JD01484, 1994. 1537

Greuell, W. and Konzelmann, T.: Numerical modeling of the energy balance and the englacial temperature of the Greenland Ice Sheet. Calculations for the ETH-Camp location (West Greenland, 1155 m a.s.l.), Global Planet. Change, 9, 91–114, doi:10.1016/0921-8181(94)90010-8, 1994. 1535

Hanna, E., Huybrechts, P., and Steffen, K.: Increased runoff from melt from the Greenland Ice Sheet: a response to global warming, J. Climate, 21, 331–341, doi:10.1175/2007JCLI1964.1, 2008. 1532

Hansen, J. and Nazarenko, L.: Soot climate forcing via snow and ice albedos, P. Natl. Acad. Sci. USA, 101, 423–428, doi:10.1073/pnas.2237157100, 2004. 1537

Kuipers Munneke, P., Van den Broeke, M. R., Lenaerts, J. T. M., Flanner, M. G., Gardner, A. S., and Van de Berg, W. J.: A new albedo parameterization for use in climate models over the Antarctic ice sheet, J. Geophys. Res., 116, D05114, doi:10.1029/2010JD015113, 2011. 1533, 1536, 1537, 1539

Lenaerts, J. T. M., van den Broeke, M. R., Déry, S. J., König-Langlo, G., Ettema, J., and Munneke, P. K.: Modelling snowdrift sublimation on an Antarctic ice shelf, The Cryosphere, 4, 179–190, doi:10.5194/tc-4-179-2010, 2010. 1535

Nick, F., Vieli, A., Howat, I. M., and Joughin, I.: Large-scale changes in Greenland outlet glacier dynamics triggered at the terminus, Nat. Geosci., 2, 110–114, doi:10.1038/NGEO394, 2009. 1532

Rignot, E., Box, J. E., Burgess, E., and Hanna, E.: Mass balance of the Greenland ice sheet from 1958 to 2007, Geophys. Res. Lett., 35, L20502, doi:10.1029/2008GL035417, 2008. 1533

Rignot, E., Velicogna, I., Van Den Broeke, M. R., Monaghan, A., and Lenaerts, J. T. M.: Acceleration of the contribution of the Greenland and Antarctic ice sheets to sea level rise, Geophys. Res. Lett., 38, L05503, doi:10.1029/2011GL046583, 2011. 1532

Simmons, A. J., Uppala, S. M., Dee, D. P., and Kobayashi, S.: ERA-Interim: new ECMWF reanalysis products from 1989 onwards, ECMWF Newl., 110, 29–35, 2007. 1535





TCD
6, 1531–1562, 2012
Albedo and SMB of Greenland
J. H. van Angelen et al.

Steffen, K. and Box, J.: Surface climatology of the Greenland ice sheet: Greenland Climate Network 1995–1999, J. Geophys. Rese., 106, 33951, doi:10.1029/2001JD900161, 2001. 1539

Stroeve, J.: Assessment of Greenland albedo variability from the advanced very high resolution radiometer Polar Pathfinder data set, J. Geophys. Res., 106, 33989—34006, doi:10.1029/2001JD900072, 2007. 1533

Stroeve, J., Box, J. E., Gao, F., Liang, S., Nolin, A., and Schaaf, C.: Accuracy assessment of the MODIS 16-day albedo product for snow: comparisons with Greenland in situ measurements, Remote Sens. Environ., 94, 46–60, doi:10.1016/j.rse.2004.09.001, 2005. 1538

Tedesco, M., Fettweis, X., Van den Broeke, M. R., Van de Wal, R. S. W., Smeets, C. J. P. P., Van de Berg, W. J., Serreze, M. C., and Box, J. E.: The role of albedo and accumulation in the 2010 melting record in Greenland, Environ. Res. Lett., 6, 014005, doi:doi:10.1088/1748-9326/6/1/014005, 2011. 1533

Van Angelen, J., van den Broeke, M., and van de Berg, W.: Momentum budget of the atmospheric boundary layer over the Greenland ice sheet and its surrounding seas, J. Geophys. Res., 116, D10101, doi:10.1029/2010JD015485, 2011a. 1535

Van Angelen, J. H., Van den Broeke, M. R., and Kwok, R.: The Greenland Sea Jet: a mechanism for wind-driven sea ice export through Fram Strait, Geophys. Res. Lett., 38, L12805, doi:doi:10.1029/2011GL047837, 2011b. 1535

Van de Wal, R. S. W., Greuell, W., Van den Broeke, M. R., Reijmer, C. H., and Oerlemans, J.: Surface mass-balance observations and automatic weather station data along a transect near Kangerlussuaq, West Greenland, Ann. Glaciol., 42, 311–316, doi:10.3189/172756405781812529, 2005. 1534

van den Broeke, M., Smeets, P., Ettema, J., van der Veen, C., van de Wal, R., and Oerlemans, J.: Partitioning of melt energy and meltwater fluxes in the ablation zone of the west Greenland ice sheet, The Cryosphere, 2, 179-189, doi:10.5194/tc-2-179-2008, 2008a. 1533, 1534, 1543

Van den Broeke, M. R., Smeets, C. J. P. P., Ettema, J., and Kuipers Munneke, P.: Surface radiation balance in the ablation zone of the west Greenland ice sheet, J. Geophys. Res., 113, D13105, doi:10.1029/2007JD009283, 2008b. 1539

Van den Broeke, M. R., Bamber, J. L., Ettema, J., Rignot, E., Schrama, E., Van de Berg, W. J., Van Meijgaard, E., Velicogna, I., and Wouters, B.: Partitioning recent Greenland mass loss, Science, 326, 984, doi:10.1126/science.1178176, 2009. 1532, 1535, 1542, 1544

Van Meijgaard, E., van Ulft, L. H., Van de Berg, W. J., Bosveld, F. C., Van den Hurk, B., Lenderink, G., and Siebesma, A. P.: The KNMI regional atmospheric climate model RACMO version 2.1, Tech. Rep. 302, Royal Netherlands Meteorological Institute, De Bilt, 2008. 1533, 1535

Warren, S. G. and Clarke, A. D.: Soot in the atmosphere and snow surface of Antarctica, J. Geophys. Res., 95, 1811–1816, doi:10.1029/JD095iD02p01811, 1990. 1537

Wientjes, I. G. M., Van de Wal, R. S. W., Reichart, G. J., Sluijs, A., and Oerlemans, J.: Dust from the dark region in the western ablation zone of the Greenland ice sheet, The Cryosphere, 5, 589–601, doi:10.5194/tc-5-589-2011, 2011. 1538

Wiscombe, W. J. and Warren, S. G.: A model for the spectral albedo of snow. I: Pure snow, J. Atmos. Sci., 37, 2712–2745, 1980. 1535, 1536

TCD
6, 1531–1562, 2012

Albedo and SMB of Greenland

J. H. van Angelen et al.





**Table 1.** Summary of the model settings applied in the different simulations with RACMO2.

| Experiment | FS Grain $m^2\,kg^{-1}$ | RF grain mm | Max liquid water | Ice Albedo | Soot ppmv |
|---|---|---|---|---|---|
| ANT | 80 | 1000 | 2 % | 0.5 | – |
| FSGRAIN | 60 | 1000 | 2 % | 0.5 | – |
| LWMAX | 60 | 1000 | C&S[1] | 0.5 | – |
| RFGRAIN | 60 | 2000 | C&S | 0.5 | – |
| ICEALB | 60 | 2000 | C&S | 0.45 | – |
| RSOOT | 60 | 2000 | C&S | 0.45 | 0.1 |
| CONTROL | 60 | 2000 | C&S | MODIS[2] | 0.1 |

[1] Maximum liquid water content based on Coléou and Lesaffre (1998).
[2] Background ice albedo based on MODIS retrievals.

**Table 2.** SMB components for different model runs, year 2007. Relative changes in parentheses.

| Experiment | Precip | Subl | Melt | Refreeze | Runoff | SMB | Melt area[1] |
|---|---|---|---|---|---|---|---|
| ANT | 713 | 27 | 340 | 156 | 242 | 444 | 9.2 % |
| FSGRAIN | 710 | 30 (+11 %) | 374 (+10 %) | 167 (+7 %) | 265 (+10 %) | 415 (−7 %) | 10.1 % |
| LWMAX | 711 | 31 (+3 %) | 406 (+9 %) | 191 (+14 %) | 271 (+2 %) | 410 (−1 %) | 11.1 % |
| RFGRAIN | 712 | 32 (+3 %) | 480 (+18 %) | 217 (+14 %) | 318 (+17 %) | 362 (−12 %) | 13.0 % |
| ICEALB | 715 | 32 (+0 %) | 503 (+5 %) | 218 (+0 %) | 341 (+7 %) | 341 (−6 %) | 13.0 % |
| RSOOT | 719 | 41 (+28 %) | 742 (+48 %) | 295 (+35 %) | 501 (+47 %) | 177 (−48 %) | 17.7 % |
| CONTROL | 720 | 42 (+2 %) | 715 (−4 %) | 297 (+1 %) | 473 (−6 %) | 205 (+16 %) | 17.4 % |

[1] Averaged melt area for the period May to Aug 2007. SSMI data gives 17.3 %.



TCD
6, 1531–1562, 2012

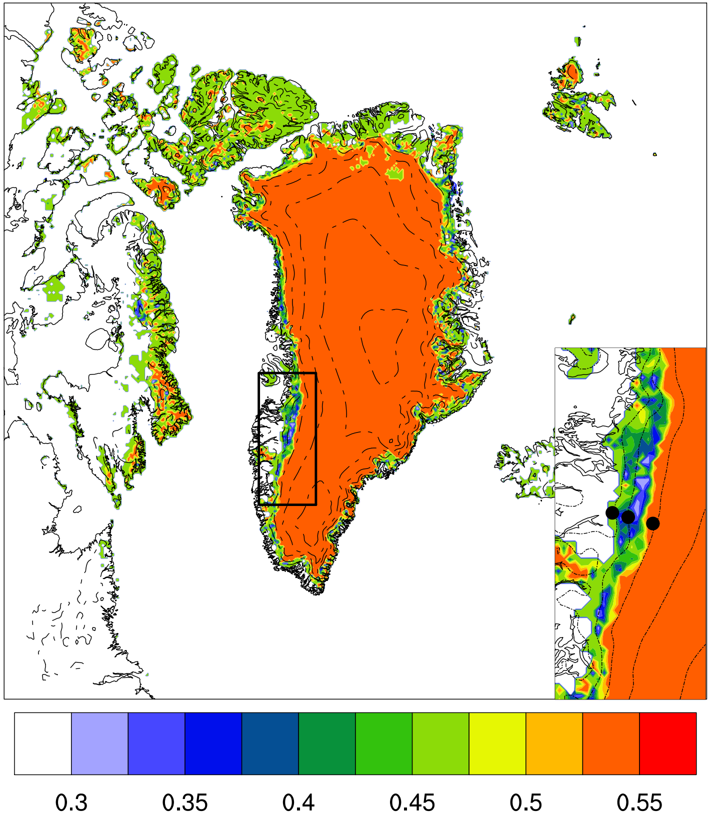


**Fig. 1.** Domain used in the RACMO2 simulations. The colors denote background ice albedo as derived from MODIS satellite data, with a fixed value of 0.55 assumed for areas currently covered by a permanent snowcover. Contour lines are at a 500 m surface elevation intervals. The area of the K-transect with the locations of the three automatic weather stations is expanded in the inset.





TCD
6, 1531–1562, 2012

**Fig. 2.** Automatic weather stations along the K-transect in West Greenland. On the left S6, on the right S9. For locations see Fig. 1. The photographs are taken at the end of August 2011.





TCD

6, 1531–1562, 2012

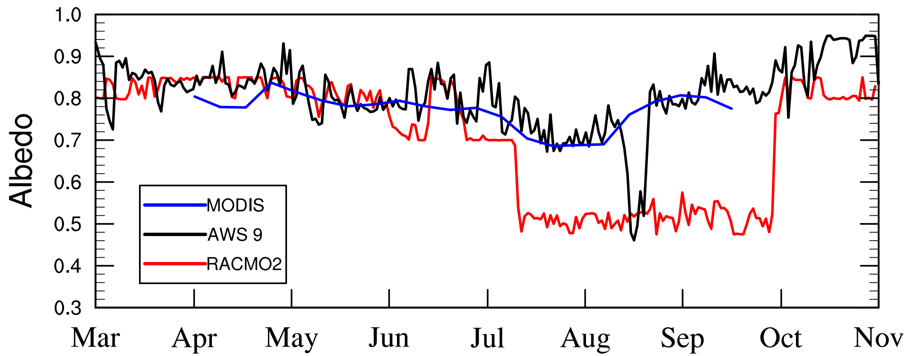


**Fig. 3.** Surface albedo for the year 2006 at S9 along the K-transect. Black line shows AWS measurements, red line shows RACMO2 results using the previous, density-dependent albedo scheme, and blue shows MODIS-derived albedo.





TCD
6, 1531–1562, 2012

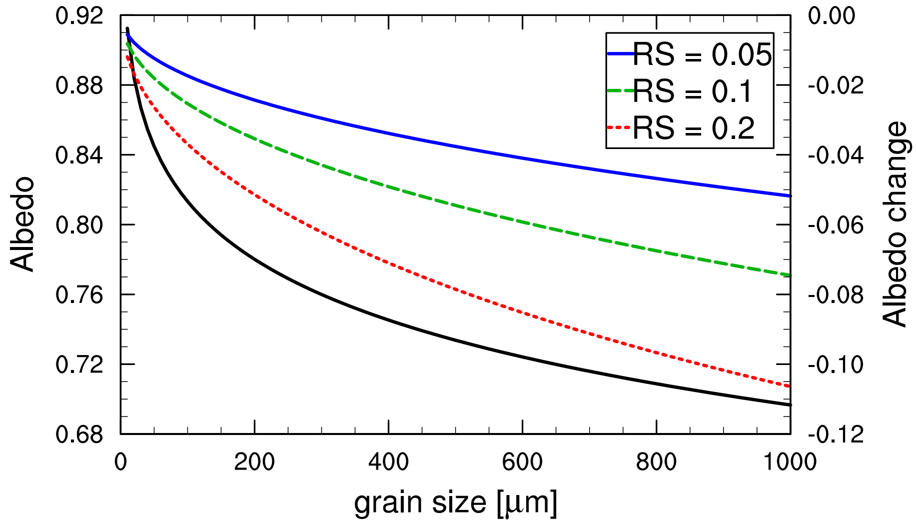


**Fig. 4.** Snow albedo as function of grain size (black, left axis) and the change of albedo as function of grain size for three different concentrations of black carbon in the snowpack: 0.05 ppmv (blue, right axis), 0.1 ppmv (green) and 0.2 ppmv (red).





TCD
6, 1531–1562, 2012

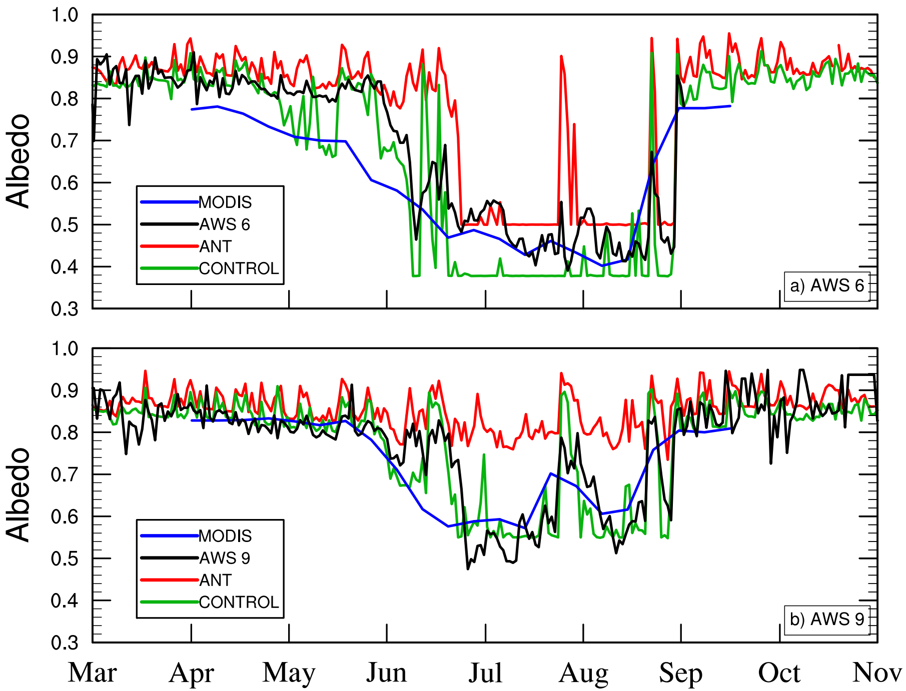


**Fig. 5.** Albedo for the year 2007 at AWS 6 (top) and AWS 9 (bottom). Black line shows AWS measurements, red line shows RACMO2 albedo in the ANT experiment, green line shows RACMO2 albedo in the CONTROL experiment and blue line shows MODIS-derived albedo.





TCD
6, 1531–1562, 2012

Albedo and SMB of Greenland

J. H. van Angelen et al.

Title Page
Abstract Introduction
Conclusions References
Tables Figures
◂ ▸
Back Close
Full Screen / Esc
Printer-friendly Version
Interactive Discussion

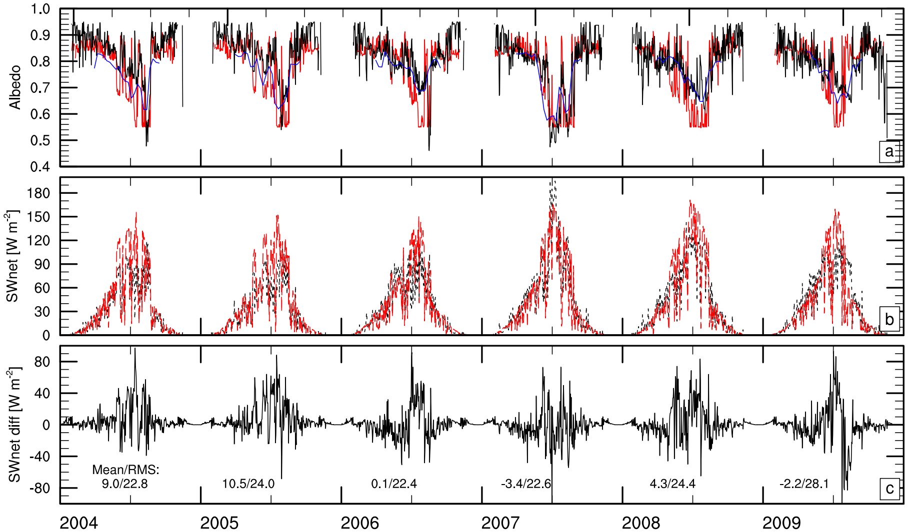


**Fig. 6.** **(a)** Albedo at location S9 for AWS data (red), MODIS observations (blue) and final (CONTROL) RACMO2 simulation (black). **(b)** Net shortwave radiation at location S9 for AWS data (red) and RACMO2 (black). **(c)** difference between RACMO2 and AWS in net short wave radiation. The numbers represent mean and root mean square difference (on a daily basis) for the individual years.

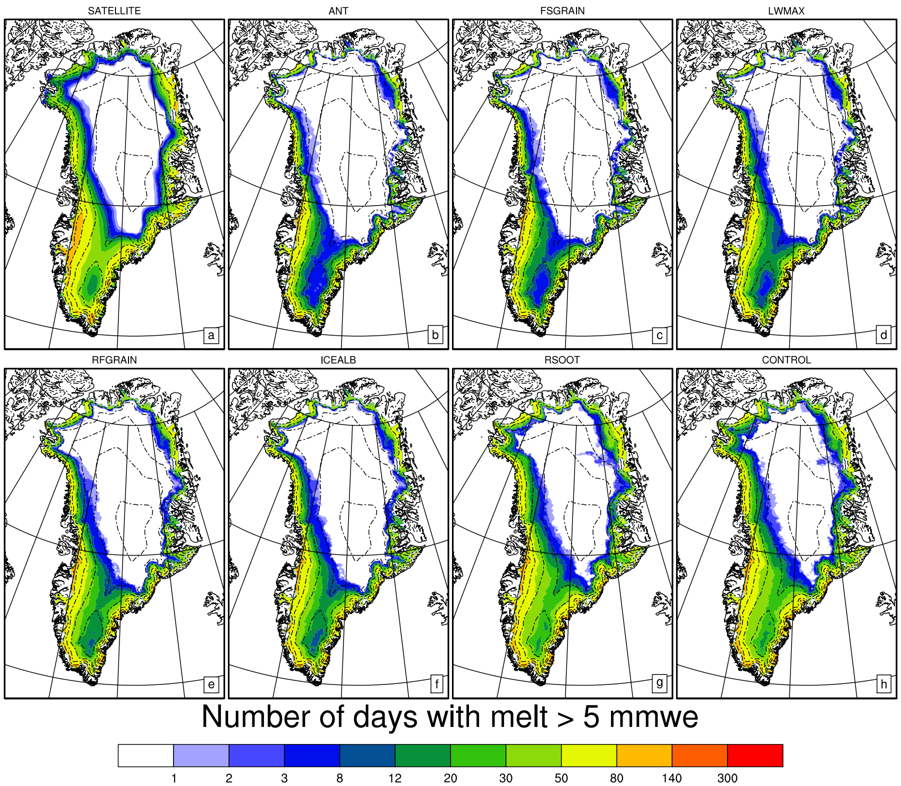


**Fig. 7.** Number of days with melt according to SSM/I satellite data **(a)** and the number of days with more than 5 mm w.e. snowmelt in the different RACMO2 experiments **(b–h)**. The individual simulations are listed in Table 1 and explained in the text. The last column in Table 2 lists the average melt area for the period May to August 2007.

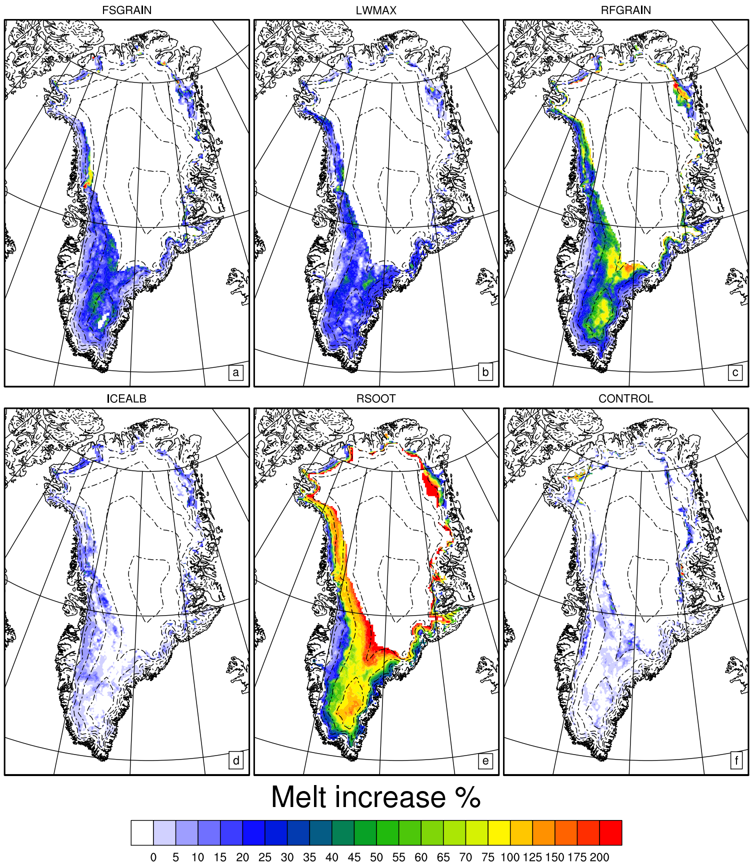


**Fig. 8.** The relative increase in snowmelt energy compared to the preceding simulation in Table 1. Panel FSGRAIN **(a)** shows the increase in snowmelt compared to the ANT simulation. As threshold a minimum of 10 mm w.e. snow melt is used.

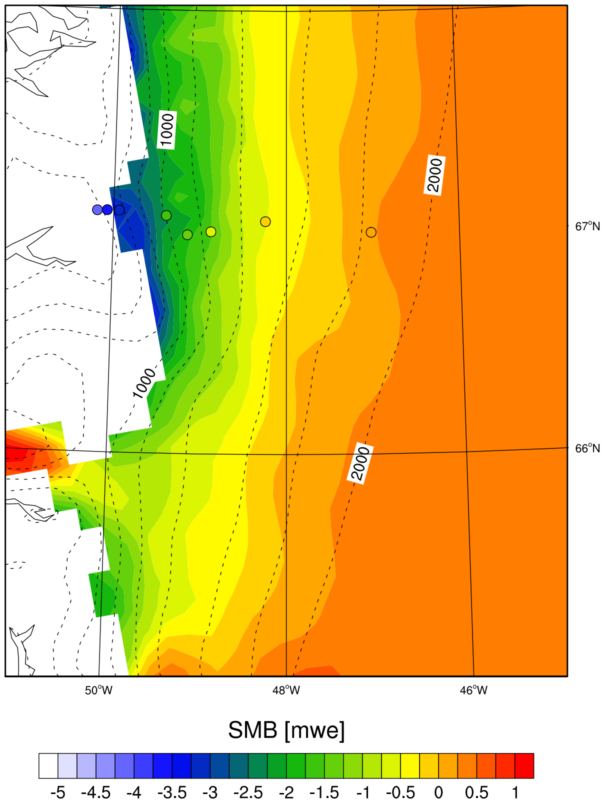


**Fig. 9.** Average surface mass balance for the period 1991–2010 in the K-transect region. The dots represent stake measurements. Height contours every 200 m.

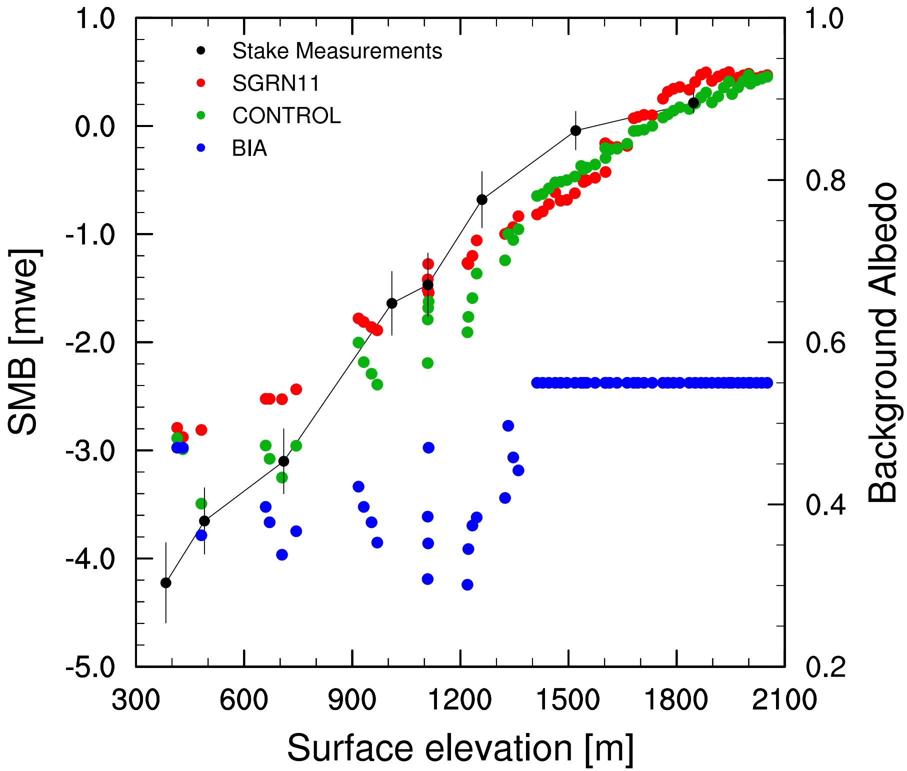


**Fig. 10.** Observed SMB along the K-transect for the period 1991–2010 with standard deviation of annual values as error bars (black); RACMO2 simulated SMB as a function of height for grid points in the K-transect region for the previous (red, Ettema et al., 2009) and new (green) albedo parameterization. Background ice albedo values (right axis) for the corresponding grid points are also shown (blue).





TCD
6, 1531–1562, 2012